JACOBS PUBLISHERS

OPEN ACCESS

Jacobs Journal of Radiation Oncology

Case Report

Pseudo-abscess Formation in a 55 Year Old Female with HPV Positive Tonsillar Squamous Cell Carcinoma: A Case Report

Jameson T. Mendel[1], MS-IV and Sun K. Yi*[2], MD

[1]Paul L. Foster School of Medicine, Texas Tech University Health Science Center, USA

[2]Department of Radiation Oncology, University of Arizona Cancer Center, USA

*Corresponding author: Dr. Sun K. Yi, M.D., 1501 N Campbell Ave, PO Box 245081 Tuscson, AZ 85724, USA, Tel: (520) 694-7236; E-mail: sunkyi@email.arizona.edu

Received: 08-04-2014

Accepted: 11-27-2014

Published: 12-05-2014

Abstract

Cystic nodal degeneration is known to be associated with HPV positive squamous cell carcinoma (SCC) of the head and neck. Differentiating between abscess formation and cystic degeneration is critical although often difficult to determine clinically. We present a case of a patient with very locally advanced HPV positive tonsillar SCC with rapidly expanding neck mass of unclear etiology. Herein we describe the potential utilization of diffusion weighted MRI for narrowing the diagnosis.

Keywords: Abscess; Radiation Therapy; Head and Neck Cancer; HPV; Tonsil

Introduction

According to the Surveillance, Epidemiology, and End Results tissue repository data, the prevalence of HPV in oropharyngeal cancers has risen by 225% from 1988 to 2004 [1]. Of all intraoral and oropharyngeal cancers, tonsillar squamous cell carcinoma (SCC) accounts for approximately 15-20% [2]. Important risk factors for the development of oropharygneal cancer include: smoking, alcohol consumption, HPV status, gender, and age. HPV positive oropharyngeal SCCs are now considered a separate subtype of SCC given their improved prognosis when compared to their HPV negative counterparts [3].

Intranodal cyst formation is commonly associated with HPV positive SCC [4]. This unique phenomenon presents as rapid neck mass enlargement at a rate greater than one would attribute to malignant growth alone. Occasionally, infection and abscess formation may mimic cystic nodal degeneration. Clinical awareness of these phenomena are important for patient management, therapeutic design, and treatment modification for patients undergoing radiation therapy (RT).

The current standard of care for patients diagnosed with stage III-IV HPV oropharyngeal SCC is chemoradiation therapy (CRT) [5]. Using computed tomography (CT), patients are simulated prior to treatment for planning purposes. Patients may be re-simulated if changes in tumor volume or anatomy occur. During treatment, patients are continually monitored with daily image guidance primarily for ensuring treatment precision, however these volumetric images may also provide additional information regarding specific anatomic changes.

Here we present a case of a patient with very locally advanced left sided HPV positive tonsillar SCC with a rapidly expanding right neck mass representing cystic nodal degeneration versus abscess formation.

Case Report

A 55 year old female with distant 15 pack-year smoking history, but otherwise insignificant past medical history, was referred to us for a left sided neck mass. The patient first noted swelling of her left neck approximately one and a half years ago. At that time, the mass was attributed to reactive lymph nodes from a viral upper respiratory tract infection (URI). She was offered further work-up upon progression of disease given high suspicion for malignancy. However she declined, opting for naturopathic treatment.

Approximately one year following initial presentation of her persistent left neck mass, the patient requested further evaluation. Diagnostic contrast-enhanced CT of the neck revealed a left tonsillar mass measuring 2.3 x 3.1cm with central ulceration and extension into the left tongue base concerning for primary malignancy. A conglomerate of ipsilateral enlarged and necrotic cervical neck lymph nodes were identified in levels II-III measuring 3.0 x 3.6cm and 2.1 x 2.0cm. A smaller subcentimeter right level II lymph node was also seen. The left tonsillar mass was biopsied and revealed basaloid SCC with immunohistochemical (IHC) staining positive for p16.

Several months following initial diagnostic neck CT, staging PET/CT scan revealed the left tonsillar mass with slight interval increase in size and an SUV of 16.1. Again seen was the left cervical adenopathy with SUV ranging from 14.6 to 16.5. A right level II lymph node was not mentioned in the original report, however in retrospect was slightly increased in size from the diagnostic study to 1.1cm with mild FDG avidity (Figure 1). Interestingly, the staging PET/CT study also identified a mass within the left nasal choana measuring 1.8cm with an SUV of 9.4. Clinically on intraoral inspection, the patient was found with a large bulky left tonsillar mass extending anteriorly onto the retromolar trigone and inferomedially into the vallecula. Neck palpation revealed a non-tender, approximately 5cm conglomerate of mobile left level II-III cervical adenopathy. There was no palpable disease in the right neck. Additionally, she reported recent onset of V2 distributed numbness over the left malar region, prompting a left nasal endoscopy which showed a crusted inferoposterior nasal choana mass correlating to the finding on PET/CT, which was discontiguous with her large left tonsillar mass. This nasal mass was biopsied and proven to be p16+ basaloid SCC, consistent with her primary tonsillar malignancy. Her case was discussed at the multidisciplinary tumor board and it was agreed upon to treat her as having locoregional disease. She was staged clinically as T4bN2cM0, stage IVb, and offered CRT definitively. In addition, the patient was formally evaluated by dentistry and cleared without need for any further dental intervention beyond routine cleaning and fluoride applications.

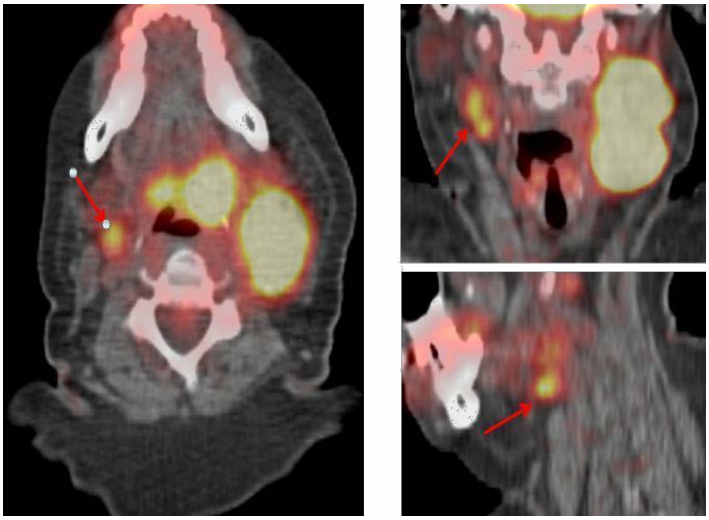

Figure 1. Representative axial, coronal, and sagittal staging PET/CT images revealing predominantly left sided disease, although a small hypermetabolic right level II node was seen (red arrows).

Due to her rapidly progressing symptoms, the patient underwent urgent CT simulation the day following her staging PET/CT. When compared with her initial diagnostic CT neck scan taken months prior, we noted enlargement of the right-sided level II neck node now measuring approximately 2cm with new evidence of central necrosis (Figure 2a). While awaiting her treatment initiation, the patient reported new URI symptoms with rapid clinical enlargement of her right neck adenopathy. Complete blood count was performed given suspicion of infection and revealed the patient to have an elevated white blood count of 15,500 cells/μL [normal ref range: 4,000-11,000 cells/μL], though she remained afebrile. Additionally, one week following CT simulation the patient underwent MRI of the face, orbits, and neck with contrast to better delineate her disease extension, which showed the enhancing left inferoposterior nasal mass with widening of the ipsilateral pterygopalatine fossa (Figure 3a). There was also dramatic enlargement of her right neck mass now measuring 3.8 cm with central necrosis and restricted diffusion (Figure 3b-c). Her RT was planned with the assistance of the diagnostic PET/CT and MRI where all gross disease with appropriate margin was planned to receive 70 Gy in 35 fractions utilizing IMRT technique, with a lower dose to elective nodal regions delivered with simultaneous integrated boost.

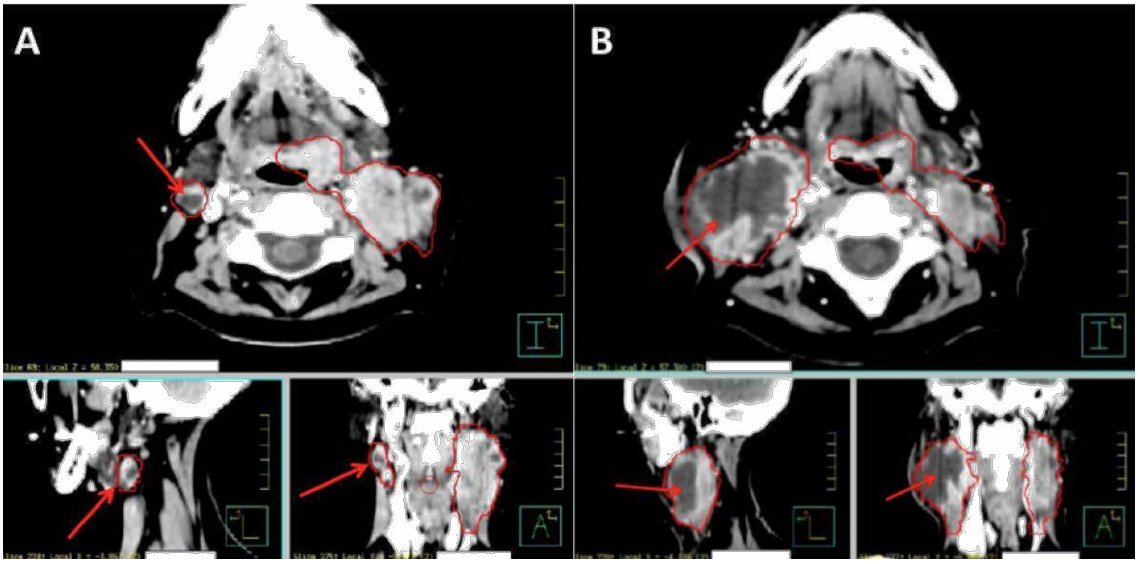

Figure 2. Representative axial, sagital, and coronal images from initial simulation. (A) and re-simulation (B) contrast enhanced CT. (a) A right cystic (approx 2cm) level II lymph node (red arrows) can be visualized on initial simulation. (b) A markedly increased rim enhancing cystic right neck mass (approx 5.7cm) is noted on re-simulation 4 weeks later, with interval response to treatment in the left neck and primary tumor.

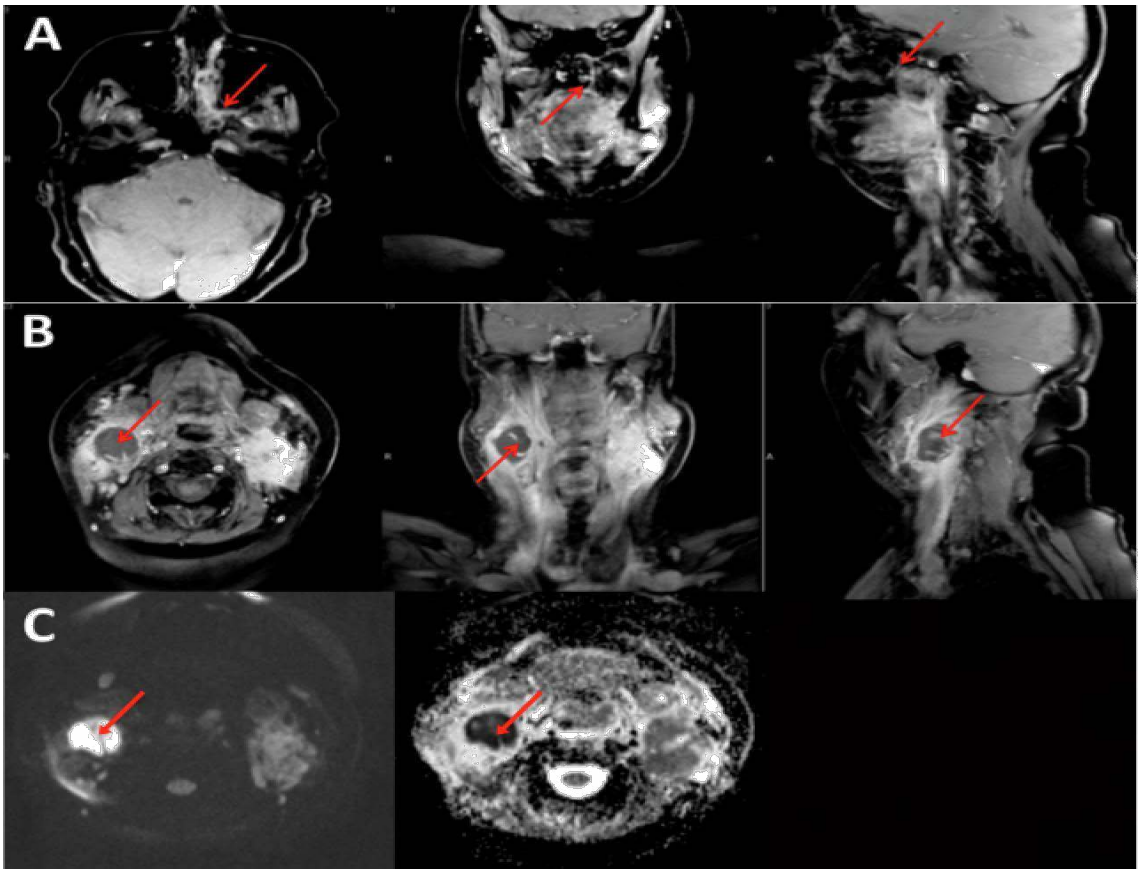

Figure 3. (a) Representative T1 post-contrast enhanced MRI images in axial, coronal, and sagital planes revealing disease extension from the left tonsil into the left inferoposterior nasal choana with widening of the left pterygopalatine fossa (red arrows); (b) Representative T1 post-contrast enhanced MRI images in axial, coronal, and sagital planes through the level of the right level II cervical lymph node revealing enlarging rim enhancing mass with hypointense center (red arrows); (c) Representative axial DWI and ADC MRI imaging revealing hyperintensity and hypointensity of the right neck mass, respectively (red arrows).

Two weeks post-simulation, the patient initiated RT with concurrent cisplatin 100 mg/m^2 given every 3 weeks. On her first fraction of RT, the patient presented with further increase in size of the right neck mass. Consequentially, the immobilization head and neck mask was difficult to utilize and was therefore modified to accommodate the enlarged right neck mass. Despite poor image registration to planned treatment volumes, RT proceeded given the rapidly progressive nature of her disease with scheduled re-simulation and re-planning.

Two weeks after initiation of CRT (RT fraction 8 of 35), the patient had continued dramatic enlargement of the right neck mass, with increasing warmth and tenderness to touch. The right neck mass was found tense and erythematous but without discrete fluctuance. The patient however remained afebrile with a white blood count within normal range. Overlying the skin of the right neck mass were multiple pustules. Incision and drainage (I&D) for culture and cytology was discussed but decided against for fear of introducing an infection not already underlying, sepsis, or tumor seeding. Instead, superficial swab of the pustules was performed and revealed 2+ gram-positive cocci with culture demonstrating Streptococcus anginosus. A ten day course of minocycline was prescribed.

On fraction 11 of 35 of RT, re-simulation CT with contrast was performed, revealing the persistently expanding right neck mass with centrally hypodense component now measuring 5.7cm compared with 2.0cm at her original simulation (Figure 2b). The differential for this mass included abscess formation versus rapidly evolving cystic malignant node. During re-planning the patient continued on with uninterrupted treatment utilizing her originally devised radiation plan. She completed the 10-day course of antibiotics and stated that her right neck mass underwent spontaneous cutaneous drainage (Figure 4). On fraction 21 of 35, daily MVCT revealed dramatic reduction of her right neck mass with spontaneous resolution of its hypodense center and marked reduction of her left sided disease as well (Figure 5).

Figure 4. Ulcerated skin overlying the right neck mass after completion of antibiotics and spontaneous drainage.

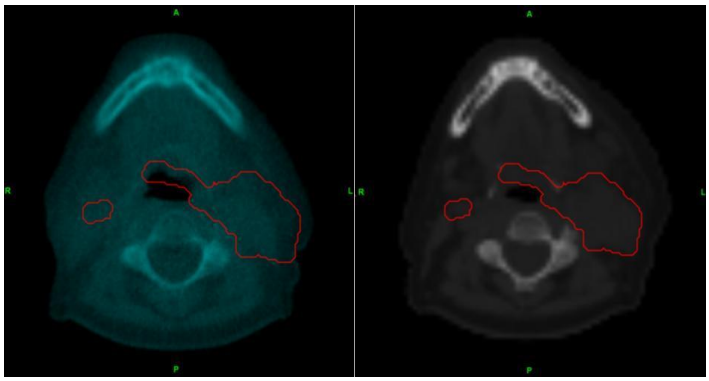

Figure 5. Daily MVCT (left in blue colorwash) taken on fraction 21 of 35, revealing spontaneously resolved right level II mass and continued decrease in size of the left-sided disease compared with the image on the right (non-contrast enhanced original CT simulation image). Red outline represents gross tumor delineated at the time of original simulation.

Over the course of treatment, the patient completed all 3 planned cycles of cisplatin chemotherapy without dose reduction and all 35 planned fractions of daily RT without interruption. She exhibited continued response of disease throughout the remaining course of treatment as determined by visual inspection, palpation, and daily image review. At the completion of treatment, she was found with near complete response of disease.

At her last follow-up, 4 months post-treatment, the patient was found with residual dysgeusia and xerostomia. On clinical examination and with endoscopic evaluation she was without gross evidence of disease. The area of spontaneous drainage along the right neck was well healed with 1cm of atrophic scar. Repeat PET/CT revealed mild residual hypermetabolic activity within the left neck with effacement of fat planes along with submucosal thickening of the left oropharynx most consistent with post-treatment changes. There was no overt evidence for recurrent disease.

Materials and Methods

Radiotherapy Planning and Treatment

Simulations were performed with Phillips Brilliance Big Bore CT scanner (Andover, MA). Head and neck aquaplast mask and bite block were utilized for immobilization and intraoral stabilization. CT images were acquired in 3mm contiguous slices from the skull vertex to mid-thorax after 100cc of ISOVUE-300 contrast was administered. All images were then imported into Philips Pinnacle v. 9.0 treatment planning software (Andover, MA) for physician contouring. Inverse planning with intensity modulated radiation therapy (IMRT)

was utilized on Tomotherapy v. 5.0 planning station (Sunnyvale, CA). The patient was treated once daily (Monday through Friday) for 35 total fractions with daily megavoltage CT image guidance on the Tomotherapy linear accelerator.

Discussion

Patterns of Extension

Although not central to our case discussion, our patient's disease revealed an unusual presentation of tonsillar cancer. It is thought that submucosal tumor extension generally follows the route of least resistance, as has been shown for nasopharyngeal carcinomas [6]. To the best of our knowledge, retrograde extension of tonsillar cancer into the nasal cavity and pterygopalatine fossa has not been previously described. Our patient's case prompted discussion as to whether her biopsy proven nasal mass represented a second primary, metastasis, or local submucosal spread, for which consensus was reached at our multidisciplinary tumor board that it represented the latter. Therefore we offered the patient definitive management with curative intent and treated her as having locoregional disease. As a consequence of her unusual disease presentation cautious treatment planning was required with both diagnostic PET/CT and MRI information.

Pseudo-abscess Formation

Patients with head and neck SCC commonly present with locally advanced disease and nodal metastases. Our patient initially presented with left-sided ipsilateral disease. A subcm right level II node seen on initial diagnostic scans showed rapid enlargement between her original simulation and 2 weeks into treatment, creating a clinical dilemma. With a near tripling in size over 4 weeks, it was unclear if we were capturing cystic changes seen with HPV related disease, or if early abscess formation was occurring. Most cervical nodal metastases associated with HNSCC never become infected. Nevertheless, Wang et al. have shown that abscess formation can be present in up to 2.3% of this patient population, particularly in those with diabetes [7]. It is believed that abscess formation within malignancy occurs as a consequence of nidus formation surrounding a focus of ulceration within a richly vascular tumor bed [8]. Our patient was not diabetic or immunocompromised, nor did she have an obvious cutaneous, mucosal, or dental source for infection.

Regardless of the underlying etiology, clinicians should hold a very low index of suspicion for deep neck infections particularly in patients undergoing chemotherapy, in order to reduce significant complications, such as sepsis, airway obstruction, mediastinitis, jugular vein thrombosis, and/or carotid artery compromise [9]. Unfortunately, due to similarities in presentation, differentiating between cystic nodal changes and abscess formation can create a diagnostic predicament for treating physicians.

While narrowing the diagnosis, abscess formation should always remain high on the differential when there is a rapidly enlarging mass with associated fever, chills, leukocytosis, fluctuance, and/or suppuration. It should be noted however, that not all patients with neck abscesses will exhibit this constellation of signs and symptoms. Our patient's lack of fever made abscess formation a less likely diagnosis, but evidence of leukocytosis kept infection a possibility. If physical examination and laboratory findings provide an ambiguous diagnosis, imaging can be of great utility.

The progression of our patient's right neck mass was temporally followed by a variety of radiographic methods with varying degrees of diagnostic specificity. Contrast enhanced CTs revealed a rim enhancing right cervical soft tissue mass with an appearance known to be associated with both abscesses and malignant cystic nodes [10] and therefore not useful in narrowing our diagnosis. Further characterization of the right neck mass by MRI showed a mass with rim enhancement, but T1 hypointense and T2 hyperintense center consistent with both cystic nodal degeneration and abscess formation [11]. There has been suggestion that MR diffusion weighted imaging (DWI) and apparent diffusion coefficients (ADC) are valuable for differentiating between abscess and necrotic tumor. The presence of central hyperintensity on DWI and low ADC values suggest abscess, while hyperintensity on both DWI and ADC is more strongly correlated with necrotic tumor [12]. Our patient's right neck mass revealed high signal on DWI and low values on ADC (Figure 3c), suggestive of abscess over cystic degeneration.

Aspiration, drainage, and culture of the right neck mass fluid would have been the gold standard for abscess diagnosis. However, this was declined by the patient for fear of introducing an infection (if not already underlying), sepsis, or tumor seeding. Therefore, overlying skin pustules were cultured instead. Though *Staphylococcus aureus* is thought to be the most common offending organism in abscesses associated with head and neck cancer [13], many are polymicrobial in nature due to proximity of the oral cavity [14]. Our patient was cultured positive for *Streptococcus anginosus* at the skin surface, an organism often considered natural flora from the gastrointestinal tract [15], associated with alcohol consumption for which our patient had a history of [16], and which has been linked to the carcinogenesis of oropharyngeal SCC [17]. Therefore, our patient's right neck mass was likely seeded from the mucosal surfaces of her upper aerodiges-

tive tract and transmitted to the skin surface by hydrostatic pressure from which it was cultured.

Treatment for neck abscesses generally consists of aspiration, I&D, and/or antibiotics. Great care must be taken with I&D or aspiration in the cervical neck due to nearby critical vascular structures. Additionally, there is also a potential for malignant seeding along the incision site or needle track [18]. Given these concerns, we decided to place our patient on antibiotics as she exhibited no clear signs of clinical deterioration. The abscess ruptured spontaneously at the skin surface and resolved shortly thereafter.

Conclusion

In patients with HPV positive SCC, cystic nodal degeneration may be difficult to differentiate from abscess formation. An accurate diagnosis is imperative as abscesses may lead to serious complications and death if left untreated. Diffusion weighted MRI may help to narrow the diagnosis. In non-critically ill patients, a course of broad spectrum antibiotics may help prevent unnecessary morbidity such as sepsis or tumor seeding associated with incision and drainage.

References

1. Chaturvedi AK, Engels EA, Pfeiffer RM, Hernandez BY, Xiao W et al. Human papillomavirus and rising oropharyngeal cancer incidence in the United States. J Clin Oncol. 2011, 29(32): 4294–4301.

2. Frisch M, Hjalgrim H, Jaeger AB, Biggar RJ. Changing patterns of tonsillar squamous cell carcinoma in the United States. Cancer Causes Control CCC. 2000, 11(6): 489–495.

3. Psyrri A, Cohen E. Oropharyngeal cancer: clinical implications of the HPV connection. Ann Oncol. 2011, 22: 997–999.

4. Goldenberg D, Begum S, Westra WH, Khan Z, Sciubba J et al. Cystic lymph node metastasis in patients with head and neck cancer: An HPV-associated phenomenon. Head Neck. 2008, 30(7): 898-903.

5. Garden AS, Asper JA, Morrison WH, Schechter NR, Glisson BS et al. Is concurrent chemoradiation the treatment of choice for all patients with Stage III or IV head and neck carcinoma? Cancer. 2004, 100(6):1171–1178.

6. Dubrulle F, Souillard R, Hermans R. Extension patterns of nasopharyngeal carcinoma. Eur Radiol. 2007, 17(10): 2622–2630.

7. Wang CP, Ko JY, Lou PJ. Deep neck infection as the main initial presentation of primary head and neck cancer. J Laryngol Otol. 2006, 120(4): 305–309.

8. Chen WT, Lee JW, Hsieh KW, Chen RF. Deep neck abscess as the predominant initial presentation of carcinoma of unknown primary: A case report. Oncol Lett. 2014, 7(4): 1297–1299.

9. Wang LF, Kuo WR, Tsai SM, Huang KJ. Characterizations of life-threatening deep cervical space infections: a review of one hundred ninety-six cases. Am J Otolaryngol. 2003, 24:111–117.

10. Yoon SJ, Yoon DY, Kim SS, Rho YS, Chung EJ et al. CT differentiation of abscess and non-infected fluid in the postoperative neck. Acta Radiol. 2013, 54(1): 48-53.

11. Wong KT, Lee YYP, King AD, Ahuja AT. Imaging of cystic or cyst-like neck masses. Clin Radiol. 2008, 63(6): 613–622.

12. Kato H, Kanematsu M, Kato Z, Teramoto T, Mizuta K et al. Necrotic cervical nodes: usefulness of diffusion-weighted MR imaging in the differentiation of suppurative lymphadenitis from malignancy. Eur J Radiol. 2013, 82(1): e28-e35.

13. Lee WC, Walsh RM, Tse A. Squamous cell carcinoma of the pharynx and larynx presenting as a neck abscess or cellulitis. J Laryngol Otol. 1996, 110(9): 893– 895.

14. Chow AW. Life-threatening infections of the head and neck. Clin Infect Dis. 1992, 14(5): 991-1002.

15. Whiley RA, Beighton D, Winstanley TG, Fraser HY, Hardie JM. Streptococcus intermedius, Streptococcus constellatus, and Streptococcus anginosus (theStreptococcus milleri group): association with different body sites and clinical infections. J Clin Microbiol. 1992, 30(1):243–244.

16. Morita E, Narikiyo M, Yokoyama A, Yano A, Kamoi K et al. Predominant presence of Streptococcus anginosus in the saliva of alcoholics. Oral Microbiol Immunol. 2005, 20(6): 362–365.

17. Shah A, Mayank M, Mulla A. Evolving role of bacteria in oral cancer. Univ Res J Dent. 2012, 2(3): 103-106.

18. Mighell AJ, High AS. Histological identification of carcinoma in 21 gauge needle tracks after fine needle aspiration biopsy of head and neck carcinoma. J Clin Pathol. 1998, 51(3): 241–243.